Continuous Multiplexed Phage Genome Editing Using Recombitrons

Authors: Chloe B. Fishman[1,#], Kate D. Crawford[1,2,#], Santi Bhattarai-Kline[1,3,#], Karen Zhang[1,2], Alejandro González-Delgado[1], Seth L. Shipman[1,4,5]*

Affiliations:

[1]Gladstone Institute of Data Science and Biotechnology, San Francisco, CA, USA

[2]Graduate Program in Bioengineering, University of California, San Francisco and Berkeley, CA, USA

[3]UCLA-Caltech Medical Scientist Training Program, David Geffen School of Medicine, University of California, Los Angeles, CA, USA

[4]Department of Bioengineering and Therapeutic Sciences, University of California, San Francisco, CA, USA

[5]Chan Zuckerberg Biohub, San Francisco, CA

[#]These authors contributed equally

*Correspondence to: seth.shipman@gladstone.ucsf.edu

ABSTRACT

Bacteriophages, which naturally shape bacterial communities, can be co-opted as a biological technology to help eliminate pathogenic bacteria from our bodies and food supply[1]. Phage genome editing is a critical tool to engineer more effective phage technologies. However, editing phage genomes has traditionally been a low efficiency process that requires laborious screening, counter selection, or *in vitro* construction of modified genomes[2]. These requirements impose limitations on the type and throughput of phage modifications, which in turn limit our knowledge and potential for innovation. Here, we present a scalable approach for engineering phage genomes using recombitrons: modified bacterial retrons[3] that generate recombineering donor DNA paired with single stranded binding and annealing proteins to integrate those donors into phage genomes. This system can efficiently create genome modifications in multiple phages without the need for counterselection. Moreover, the process is continuous, with edits accumulating in the phage genome the longer the phage is cultured with the host, and multiplexable, with different editing hosts contributing distinct mutations along the genome of a phage in a mixed culture. In lambda phage, as an example, recombitrons yield single-base substitutions at up to 99% efficiency and up to 5 distinct mutations installed on a single phage genome, all without counterselection and only a few hours of hands-on time.

INTRODUCTION

Bacteriophages (phages) naturally control the composition of microbial ecosystems through selective infection of bacterial species. Humans have long sought to harness this power of phages to make targeted interventions to the microbial world, such as delivering phages to a patient suffering from an infection to eliminate a bacterial pathogen. This approach to mitigate pathogenic bacterial infections, known as phage therapy, predates the discovery of penicillin, with 100 years of evidence for efficacy and safety[4]. However, the success of small molecule antibiotics over the same period of time has overshadowed and blunted innovation in phage therapy.

Unfortunately, it is now clear that reliance on small molecule antibiotics is not a permanent solution. Antimicrobial resistance in bacteria was associated with between 1–5 million deaths worldwide in 2019[5], a figure that is projected to rise in the coming decades[6]. As such, there is a pressing need for alternatives or adjuvants to small-molecule antibiotics, like phage therapy, to avoid returning to the rampant morbidity of bacterial infections of the pre-antibiotic era. This work has already begun, with researchers and clinicians utilizing phage screening pipelines to identify natural phages for use in patients to overcome antimicrobial-resistant infections[7,8].

While these efforts demonstrate the potential of phage therapeutics, they do not scale well. Screening natural phages for each patient is time- and effort-intensive, requires massive repositories of natural phages, and results in the clinical use of biological materials that are not fully characterized[1]. To functionally replace or supplement small-molecule antibiotics, phage therapy needs to be capable of industrialization and more rapid iteration. This will likely include modifying known phages to create engineered therapeutic tools that target specific pathogens and evade natural bacterial immunity, rather than just the opportunistic isolation of natural phages. However, such approaches are limited by the relative difficulty in modifying phage genomes[1].

The various approaches to modify phage genomes and the limitations imposed by each have been recently reviewed[2]. One approach is to modify phage genomes by recombination within their bacterial host, which is inefficient and requires laborious screening of phage plaques.

44 That screening effort can be reduced by imposing a counterselection on the unedited phage, such

45 as CRISPR-based depletion of the wild-type phage[9-12]. However, this negative selection is not

46 universally applicable to all edit types because it requires functional disruption of a protospacer

47 sequence[13]. Phages also frequently escape CRISPR targeting[14], which can result in most

48 selected phages containing escape mutations outside of the intended edit[9]. Another approach is

49 to "reboot" a phage by assembling a modified phage genome *in vitro* and repackaging it in a

50 host[15], but such rebooting requires extensive work to enable *in vitro* assembly of a phage genome,

51 and phage genome size limits the efficiency of transformation. A fully cell-free packaging system

52 eliminates the issue of inefficient transformation[16], but instead requires substantial upfront

53 technical development, which is host species-specific.

54 Because of the urgent need for innovation in phage therapeutics and the clear technical

55 hurdle in modifying phage genomes, we developed an alternative system for phage engineering.

56 Our system edits phage genomes as they replicate within their bacterial hosts, by integrating a

57 single-stranded DNA (ssDNA) donor encoding the edit into the replicating phage genome using

58 a single-stranded annealing protein (SSAP) and single-stranded binding protein (SSB). A critical

59 innovation is that we use a modified bacterial retron[17-20] to continuously produce the editing

60 ssDNA donor by reverse transcription within the host. Thus, propagating a population of phage

61 through this host strain enables continuous accumulation of the intended edit over generations

62 within a single culture.

63 Moreover, this system enables a more complex form of editing in which the bacterial

64 culture is composed of multiple, distinct editing hosts, each producing donors that edit different

65 parts of the phage genome. Propagation of phages through such a complex culture leads to the

66 accumulation of multiple distinct edits at distant locations in individual phage genomes. Here, we

67 demonstrate this approach, showing that (1) the editing is a continuous process in which edits

68 accumulate over time; (2) it can be applied to multiple types of phage and used to introduce

69 different edit types; (3) it can be optimized to reach efficiencies that do not require

70   counterselection; and (4) it can be used to make multiplexed edits across a phage genome. For

71   disambiguation with other techniques, we call this approach *phage retron recombineering*, and

72   term the molecular components that include a modified retron a *recombitron*.

73   **RESULTS**

74   **Recombitrons Target Phage Genomes for Editing**

75   There are four core molecular components of a recombitron: a retron non-coding RNA

76   (ncRNA) that is modified to encode an editing donor; a retron reverse transcriptase (RT); a single-

77   stranded binding protein (SSB); and a single-stranded annealing protein (SSAP) (**Fig 1a**).

78   Endogenous retrons partially reverse transcribe a short (~200 base) ncRNA into a single-stranded

79   reverse-transcribed DNA (RT-DNA) of ~90 bases. In bacteria, this RT-DNA is used in conjunction

80   with retron accessory proteins to detect and respond to phage infection. The retron accessory

81   proteins are necessary for the phage defense phenotype and are not included in the recombitron

82   to avoid reconstituting an anti-phage system[21-24]. We modify the retron ncRNA by adding

83   nucleotides to the region that is reverse transcribed that are homologous to a locus in the phage

84   genome and carry the edit we aim to incorporate.

85   The recombitron we begin with here specifically contains a modified retron-Eco1 ncRNA

86   expressed on the same transcript as a retron-Eco1 RT, which will produce a 90-base-long

87   reverse-transcribed editing donor (RT-Donor) inside the host bacteria. Once produced, the SSB

88   will bind the editing RT-Donor to destabilize internal helices and promote interaction with an

89   SSAP. In this case, we leverage the endogenous *E. coli* SSB. Next, an SSAP promotes annealing

90   of the RT-Donor to the lagging strand of a replication fork, where the sequence is incorporated

91   into the newly replicated genome[25]. From a separate promoter, we express the SSAP CspRecT

92   along with an optional recombitron element mutL E32K, a dominant-negative version of *E. coli*

93   mutL that suppresses mismatch-repair[26-28]. Such suppression is necessary when creating single-

94   base mutations, but not required for larger insertions or deletions.

95   This system benefits from stacking several beneficial modifications to the retron and

96   recombineering machinery discovered previously. The retron ncRNA, in addition to being modified

97   to encode an RT-Donor, is also modified to extend the length of its a1/a2 region, which we

98   previously found to increase the amount of RT-DNA produced[20,29]. The SSAP, CspRecT, is more

99   efficient than the previous standard, lambda β, and is known to be compatible with *E. coli* SSB[27].

100   The dominant-negative mutL E32K eliminates the requirement to pre-engineer the host strain to

101   remove mutS[26,30]. A previous study attempted a single edit using a retron-produced donor against

102   T5 phage, but only reported editing after counterselection[12]. By using these stacked innovations,

103   we aim to produce a system that does not require counter selection.

104   To test whether recombitrons can be used to edit phages, we designed recombitrons

105   targeting 5-7 sites across the genome of four *E. coli* phages: Lambda, T7, T5, and T2. Each

106   recombitron was designed to make synonymous single-base substitutions to a stop codon, which

107   we assume to be fitness neutral. We constructed separate recombitrons to produce the RT-Donor

108   in either of the two possible orientations, given that the mechanism of retron recombineering

109   requires integration into the lagging strand, and created a recombitron with a catalytically-dead

110   RT at one position per phage as a control. We pre-expressed the recombitron for 2 hours in BL21-

111   AI *E. coli* that lack the endogenous retron-Eco1, then added phage at an MOI of 0.1 and grew the

112   cultures for 16 hours overnight. The next day, we spun down the cultures to collect phage in the

113   supernatant. We used PCR to amplify the regions of interest in the phage genome (~300 bases)

114   surrounding the edit sites. We sequenced these amplicons on an Illumina MiSeq and quantified

115   editing with custom software.

116   We observed RT-dependent, counter-selection-free editing in lambda (~20%), T7

117   (~1.5%), and T5 (~0.6%) (**Fig 1b-d**). We did not observe editing in T2 above the dead RT

118   background level, which could be due to T2's use of modified 5-hydroxymethycytosines

119   (**Supplementary Fig 1a**)[31]. In lambda, T7, and T5, we obtained similar maximum editing

120   efficiencies at each site across the genome. Editing efficiency was affected by RT-Donor direction

121   in a manner generally consistent with individual phage replication mechanisms. Lambda has an

122   early bidirectional phase of replication and a later unidirectional phase[32]. Thus, either strand may

123   be lagging at some point and, accordingly, we observed similar efficiencies for the forward and

124   reverse recombitron (**Fig 1b**). T7 has a single origin of replication at one end of its linear genome,

125   and we observed directional editing favoring the predicted lagging (reverse) strand (**Fig 1c**)[33].

126   Interestingly, T5 replication is less well studied, with one report describing bidirectional replication

127   from multiple origins[34]. However, we found a clear strand preference indicating dominant

128   unidirectional replication from one end of the phage genome (**Fig 1d**).

129   Editing efficiency differed among the phages tested, with lambda being the most efficiently

130   edited. One possible explanation for this difference is that lambda is the only temperate phage

131   tested, so hypothetically the editing could be occurring while lambda was integrated into the *E.*

132   *coli* genome. However, we obtained two results inconsistent with this hypothesis. First, we

133   generated a lambda strain with an inactivated cI gene (ΔcI) that is required for prophage

134   maintenance, and found similar levels of editing in that lambda strain as compared with our

135   standard lambda strain (**Supplementary Fig 1b**)[35]. Next, we modified the bacterial host to remove

136   the lambda prophage integration site (attB), and again found similarly high levels of editing of the

137   ΔcI strain in the attB⁻ bacteria (**Supplementary Fig 1b**)[36]. Another possibility is that lambda β, an

138   SSAP encoded by lambda, assists the recombitron[25]. However, we found no editing of lambda in

139   the absence of CspRecT expression, which is inconsistent with that possibility (**Supplementary**

140   **Fig 1c**). Perhaps the recombitron differentially affects phage replication, which in turn affects

141   editing efficiency. However, we found no effect on replication of any phage (as measured by

142   phage titer) when the recombitron was included or expressed in the phage's bacterial host

143   (**Supplementary Fig 1d,e**).

144   Another alternative explanation is SSB compatibility[37]. Phage T7, unlike lambda, encodes

145   a separate SSB in its genome (gp2.5)[38]. Perhaps T7 SSB competes with the *E. coli* SSB for the

146   recombitron RT-DNA, which could inhibit interactions with the CspRecT. To test this possibility,

147 we repeated the lambda and T7 editing experiments at one locus each, while overexpressing

148 either the *E. coli* or the T7 SSB. Consistent with this explanation, we found that overexpression

149 of the T7 SSB has a large negative impact on editing of lambda, while the *E. coli* SSB had a much

150 smaller impact (**Fig 1e**). We similarly found that overexpression of the T7 SSB strongly reduced

151 editing of T7, whereas overexpression of the E. coli SSB had a large positive effect on T7 editing,

152 more than doubling the efficiency to a rate of 10% (**Fig 1f**). Thus, the T7 SSB appears to inhibit

153 the retron recombineering approach, but can be counteracted by overexpressing a compatible

154 SSB. We tried a similar approach with T5, which has a much less characterized SSB (PC4-like,

155 by homology to phage T4[39]). While the T7 SSB similarly inhibited T5 editing, the T5 PC4-like

156 protein had a small negative effect on editing, and the *E. coli* SSB did not improve T5 editing

157 (**Supplementary Fig 1f-h**).

158

159 **Continuous Editing**

160 One clear advantage of using recombitrons for phage editing is the fact that they edit

161 continuously while the phage is propagating through the culture, increasing the proportion of

162 edited phages with every generation (**Fig 1g**). This is quite distinct from other methods of

163 recombineering in phages where materials are delivered via transformation of the host at a single

164 point in time[40]. To illustrate the continuous nature of this approach, we edited lambda over three

165 rounds of culture. Editing and analysis was performed as described above, but at the end of each

166 round of editing, we propagated the resulting phage population through a fresh culture of editing

167 the host. The percentage of edited genomes increased with each additional round, reaching >80%

168 of phages edited after three rounds (**Fig 1h**).

169
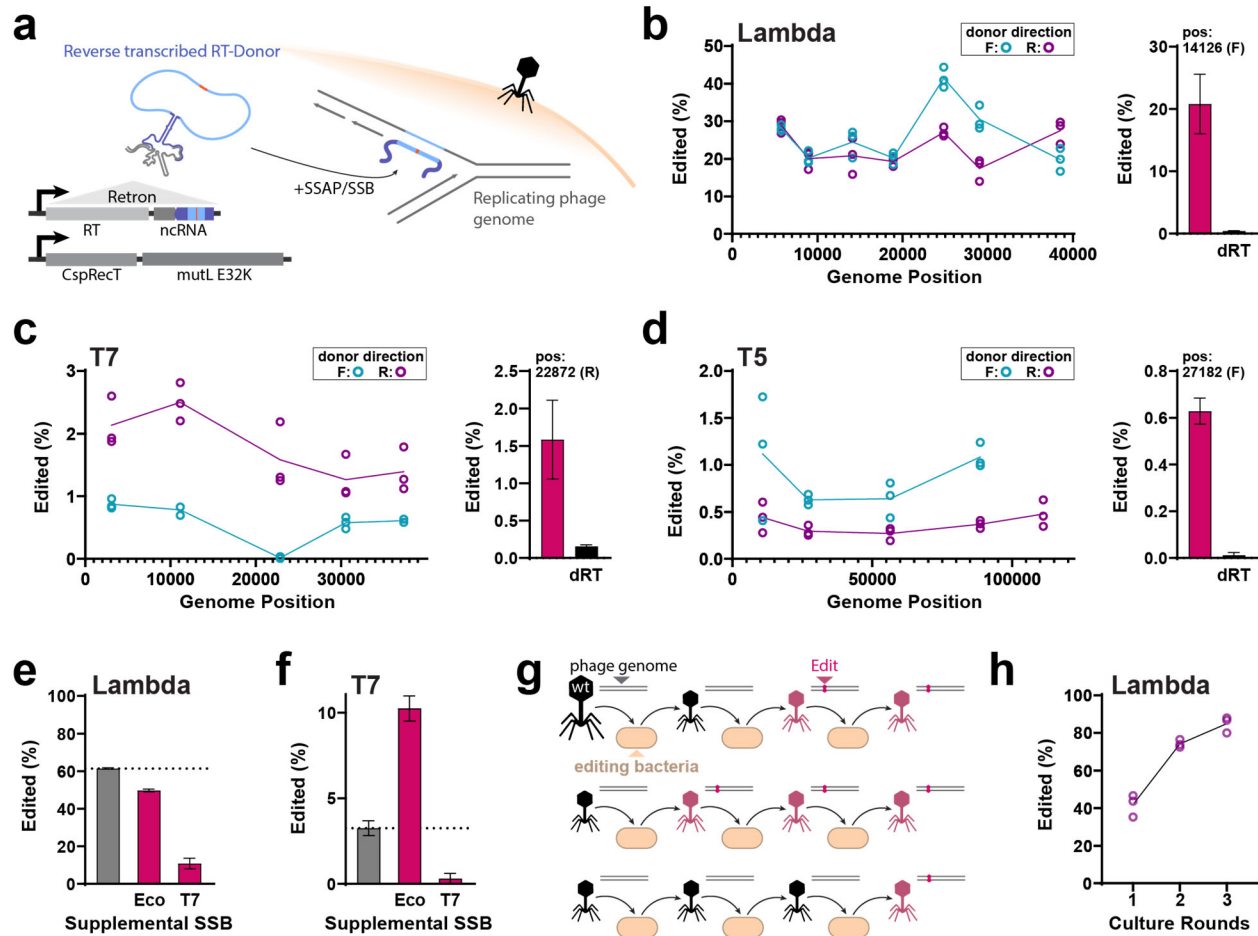
Figure 1. Recombitrons Target Phage Genomes for Continuous Editing a. Recombitron schematic: a modified retron generates ssDNA containing a donor sequence with an edit flanked by homology to the phage genome that is integrated into the phage genome during replication by SSB and SSAP. The retron cassette is expressed from an operon containing a reverse transcriptase (RT) and ncRNA. The reverse-transcribed region of the ncRNA is shown in purple with an inserted donor sequence in light blue, and the edit site is shown in orange. A second operon expresses CspRecT and mutL E32K. **b.** Left: Edited phage genomes (as a % of all genomes) across lambda phage. Editing with a forward RT-DNA is shown in blue, reverse in purple. Three individual replicates are shown in open circles at each point. Right: Editing with the recombitron at site 14,126 (±SD) is significantly greater than editing with a dRT control (t-test, *P*=0.0018). **c.** Left: Edited phage genomes across phage T7 for three replicates at each position, displayed as in b. Right: Editing with the recombitron at site 22,872 (±SD) is significantly greater than editing with a dRT control (t-test, *P*=0.0094). **d.** Left: Edited phage genomes across phage T5 for three replicates at each position, displayed as in b. Right: Editing with the recombitron at site 27,182 (±SD) is significantly greater than editing with a dRT control (t-test, *P*<0.0001). **e.** Editing of lambda at site 30,840 (F) (±SD) compared to editing with supplemental expression of *E. coli* SSB or T7 SSB. There is a significant effect of SSB expression (one-way ANOVA, *P*<0.0001, N=3), with both the *E. coli* (*P*=0.005) and T7 (*P*=<0.0001) significantly different than the no SSB condition (Dunnett's, corrected). **f.** Editing of T7 at site 11,160 (R) (±SD) compared to editing with supplemental expression of *E. coli* SSB or T7 SSB. There is a significant effect of SSB expression (one-way ANOVA, *P*<0.0001, N=3), with both the *E. coli* (*P*=0.0002) and T7 (*P*=0.0127) significantly different than the no SSB condition (Dunnett's, corrected). **g.** Schematic illustrating the accumulation of edited phages with multiple rounds of editing. **h.** Proportion of edited lambda phage

193   increases over 3 rounds of editing of lambda at site 30,840 (F). Three replicates per round are shown in
194   open circles. Additional statistical details in Supplementary Table 1.

195

196

197   **Optimizing Recombitron Parameters**

198   Given the initial success of recombitrons, we next tested the parameters of the system to

199   achieve optimal editing. The first parameter we tested was length of the RT-Donor. We designed

200   a set of recombitrons with different RT-Donor lengths, each encoding a lambda edit (C14070T) in

201   the center of the homologous donor (**Fig 2a**). We found no editing with a 30 base RT-Donor, but

202   all other lengths tested from 50 to 150 bases produced successful editing (**Fig 2b**). The highest

203   overall editing rates occurred with a 70 base RT-Donor. However, for donors between 50 and 150

204   bases, an analysis corrected for multiple comparisons only found a significant difference between

205   a 70 and 150 base donors, indicating that long RT-Donor length is detrimental to editing efficiency

206   (**Fig 2b**).

207   The next parameter we tested was positioning of the edit within the RT-Donor. We tested

208   a set of recombitrons where we held a 90 base region of homology to lambda constant and

209   encoded an edit at different positions along the donor, each of which introduce a distinct

210   synonymous single-base substitution (**Fig 2c**). Here we found that the editing rate increased as

211   the edit approached the center of the donor (**Fig 2d**). After correcting for multiple comparisons,

212   we found no difference between edit placement between a central 27 bases from position 37 to

213   64, but a significant decline in editing outside the central region.

214   We also tested the effect of position when encoding multiple edits on a single RT-Donor.

215   In this case, we tested a set of recombitrons with edits at different positions along the RT-Donor

216   as above, but additionally included a central edit on every RT-Donor (**Fig 2e**). Similar to the effect

217   above, we found that the rate of incorporating both of the edits on a single phage genome declined

218   as the scanning edit approached either edge of the RT-Donor (**Fig 2f**). However, there was a

219   consistent editing rate for all recombitrons in phage genomes that were only edited at the central

220   site. When both edits were positioned toward the center of the donor, most genomes contained

221 both edits, whereas when the scanning edit was positioned toward the edge of the RT-Donor,

222 there was a significant increase in likelihood of incorporating only the central edit (**Fig 2f**). We

223 interpret this result as evidence that the RT-Donor can be partially used, with a bias toward using

224 the central part of the RT-Donor. We also found only a very low rate of the scanning edit being

225 incorporated without the central edit (**Supplementary Fig 2**).

226 Next, we tested the effect of increasing the number of edits per recombitron. We

227 constructed a set of recombitrons with 3, 7, 9, or 11 of the scanning edits used above (**Fig 2g**).

228 We found that editing with the 3-edit recombitron was comparable to the single edits we previously

229 tested, but editing rates declined across all edit sites when additional edits were encoded on a

230 single recombitron (**Fig 2h**). We interpret this as an effect of decreasing homology across the

231 donor, making it more difficult to anneal to the target site. To further assess which edits on the

232 same RT-Donor were likely to be acquired together, we analyzed the co-occurrence of edits.

233 Because of the effect of decreasing homology on the editing rate, we calculated the correlation

234 coefficient r^2 and normalized it to the overall editing rate for each donor at each site. We found

235 that there was a bias toward acquiring the more central edits overall, and a tendency to co-edit

236 nearby sites (**Fig 2i**), again supporting the potential for partial use of the RT-Donor.

237

238 **Optimizing host strain**

239 We also tested the effect of the editing host. Specifically, we compared editing in: B-strain *E. coli*

240 (BL21-AI); a derivative of BL21-AI lacking the endogenous retron-Eco1; K-strain *E. coli* (MG1655);

241 and derivative of MG1655 lacking Exo1 and RecJ – nucleases whose removal was previously

242 shown to increase recombination rates using synthetic oligonucleotides[18,41]. We found no

243 difference between the BL21-AI and retron-deletion derivative, indicating that the endogenous

244 retron does not interfere with the recombitron system (**Fig 2j**). We found decreased editing in the

245 wild-type K-strain that was not statistically significant as compared to the B-strain, but significantly

246 improved editing in the modified K-strain versus the B-strain (**Fig 2j**).

247
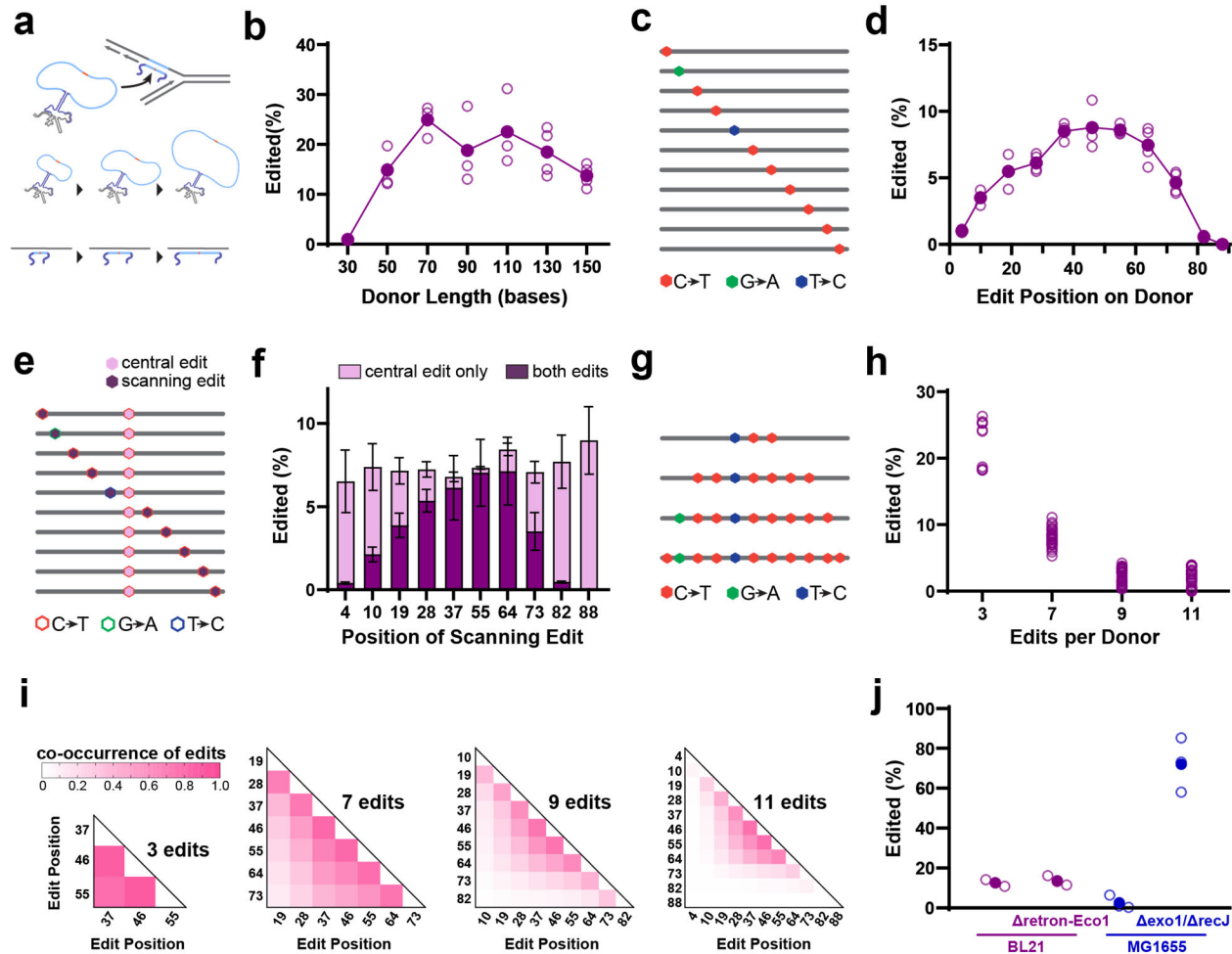
Figure 2. Optimizing Recombitron Parameters with Lambda Phage. a. Schematic of recombitron with longer and shorter RT-Donors, with more or less homology to the genome surrounding the edit site. **b.** Editing (%) of lambda with donors ranging in size from 30-150 bases. Three to four biological replicates are shown in open circles and closed circles show the average per recombitron, demonstrating an effect of length (one-way ANOVA, $P<0.0001$). All RT-Donors greater than 50 bases yield significantly improved editing from a 30 base donor (Sidak's corrected, $P<0.05$), and a RT-Donor of 150 bases is significantly worse than 70 bases (Sidak's corrected, $P<0.05$). **c.** Schematic of RT-Donors with homology to a single lambda region, each containing a scanning edit. **d.** Editing (%) of lambda with donors containing scanning edit. Four biological replicates are shown in open circles and closed circles show the average per recombitron, demonstrating an effect of edit placement (one-way ANOVA, $P<0.0001$). Edit placement at positions ≤28 or ≥73 is significantly worse position 46 (Dunnett's corrected, $P<0.001$). **e.** Schematic of RT-Donors containing the scanning edit with an additional, constant central edit. **f.** Editing (%) of lambda with donors containing both the scanning and central edits. Editing rate when only the central edit is acquired is shown in light pink, acquisition of both edits shown in purple (±SD). Position of scanning edit does not affect total editing (one-way ANOVA, $P=0.7868$), but does affect whether both edits are installed (one-way ANOVA, $P<0.0001$). **g.** Schematic of multi-edit recombitrons containing 3, 7, 9, and 11 edits per RT-Donor. **h.** Editing (%) of lambda from the multi-edit recombitrons, each site across three to four biological replicates is shown as an open circle. Number of edits per RT-Donor significantly affects average editing rate across sites (one-way ANOVA, $P<0.0001$), with 7, 9, and 11 edits all performing significantly worse than 3

267 (Dunnett's corrected, *P*<0.0001). **i.** Co-occurrence of edits that are acquired from multi-edit donors.
268 Heatmap shows correlation coefficient r^2, normalized to the overall editing rate for each donor at each
269 site. **j.** Editing (%) of lambda in different host strains at position 14,126 (R), using a plac-recombitron that is
270 functional across all strains. Three biological replicates are shown as open circles and the average is shown
271 as a closed circle. There is a significant effect of strain (one-way ANOVA, *P*<0.0001). The MG1655 (exo1-
272 /recJ-) strain yielded significantly more editing than the BL21 (Dunnett's corrected, *P*<0.0001). Additional
273 statistical details in Supplementary Table 1.
274
275
276 **Insertions and Deletions via Recombitrons**

277 Genomic deletions and insertions are also useful for engineered phage applications.

278 Deletions can be used to remove potential virulence factors or eukaryotic toxins from phage

279 genomes or to optimize phages by minimization. Insertions can be used to deliver cargo, such as

280 nucleases that can help kill target cells, or anti-CRISPR proteins to escape phage defense

281 systems. Therefore, we tested the efficiency of engineering deletions and insertions of increasing

282 size into the lambda genome.

283 We began by comparing the efficiency of deleting 2, 4, 8, 16, or 32 bases to one of the

284 single base synonymous substitutions we tested previously (**Fig 3a**). These experiments were

285 performed in the engineered K-strain that we found to yield higher editing efficiencies using

286 inactivated cI lambda as the phage. We deleted bases preceding position 37,673 using

287 recombitrons where a 90 base RT-Donor contained flanking homology around the deletion site,

288 but omitted the bases to be deleted. We found consistent editing of ~45% for each of the deletions

289 (**Fig 3b**) using Illumina amplicon sequencing. The deletion size did not significantly affect the

290 efficiency of editing, although all the deletions exhibited significantly lower editing than the

291 synonymous single base substitution.

292 We next tested insertion of 2, 4, 8, 16, or 32 bases into the same lambda site (**Fig 3c**).

293 Here, we found a range of editing efficiencies, from ~32% for insertions of 2 bases to ~10% for

294 insertions of 16 bases (**Fig 3d**). Like the deletions, all insertions were significantly less efficient

295 than a synonymous single base substitution. Unlike the deletions, insertion size significantly

296 affected efficiency, favoring smaller insertions.

297 Whereas the synonymous single base substitution is assumed to be neutral for phage

298 fitness, we cannot assume the same for the deletions and insertions, which could affect

299 transcription or phage packaging. This may underlie the lower, although still substantial, rate of

300 deletions and insertions overall. Additionally, the PCR required for analysis of editing by amplicon

301 sequencing is known to be biased toward smaller amplicons, which could inflate the measured

302 rates of the larger deletions and decrease the measured rates of larger insertions.

303 To test yet larger insertions in a manner that is not subject to the size bias of PCR, we

304 edited phages and then sequenced their genomes without amplification using long-read nanopore

305 sequencing (**Fig 3e**). After editing, we isolated phage genomes via Norgen Phage DNA Isolation

306 kit, attached barcodes and nanopore adapters, and sequenced molecules for 24-48h on a MinION

307 (Oxford Nanopore Technologies). We quantified the resulting data using custom analysis software

308 that binned reads by alignments to three possible genomes: a wild-type lambda genome, a

309 lambda genome containing the relevant edit, or the BL21 *E. coli* genome as a negative control.

310 BLAST alignment scores (percent identity, e-value, and alignment length) were compared for any

311 read aligning to the lambda genome (wild-type or edited) in the region of the intended edit to

312 quantify wild-type versus edited genomes. Consistent with a PCR bias for size, we found that

313 amplification-free sequencing resulted in comparable editing rates to amplification-based

314 sequencing for quantifying a single base substitution, but slightly lower rates of editing when

315 measuring a 32 base pair deletion as compared to amplification-based sequencing

316 (**Supplementary Figure 3a**).

317 This amplification-free sequencing approach enabled us to extend our deletion and

318 insertion size ranges. For deletions, we tested 32, 64, 100, 300, or 500 base pairs. We found

319 deletions of 32 bases at a frequency of ~23%, 300 bases at a frequency of ~2.7%, and 500 bases

320 at a frequency of 0.16% (**Fig 3f**). We did not observe deletions of 64 or 100 bases in our data.

321 However, our long-read coverage of the editing region in these samples was limited, so we can

322 only conclude that, if these edits occur, they are present at <1.8% and <1% respectively across

323   the three replicates of our sequencing data (**Supplementary Figure 3b,c**). In cases where we

324   observe deletions, they were reliably found at the intended location and of the intended size

325   (**Supplementary Figure 3e**).

326   We also tested insertion of larger sequences. We built recombitrons to insert a 34 base frt

327   recombination site, a 264 base anti-CRISPR protein (AcrIIA4), a 393 base anti-CRISPR protein

328   (AcrIIA13), and a 714 base sfGFP. As anticipated from the low insertion rates of insertions >8

329   base pairs, we did not observe any of these larger insertions in our long-read sequencing data,

330   which was read-limited to a detection level of ~1% (**Supplementary Figure 3d**). Thus, the

331   recombitrons enable high efficiency deletions of up to 32 base pairs and insertions of up to 8 base

332   pairs, but are not practical for counterselection-free isolation of larger deletions or insertions.

333
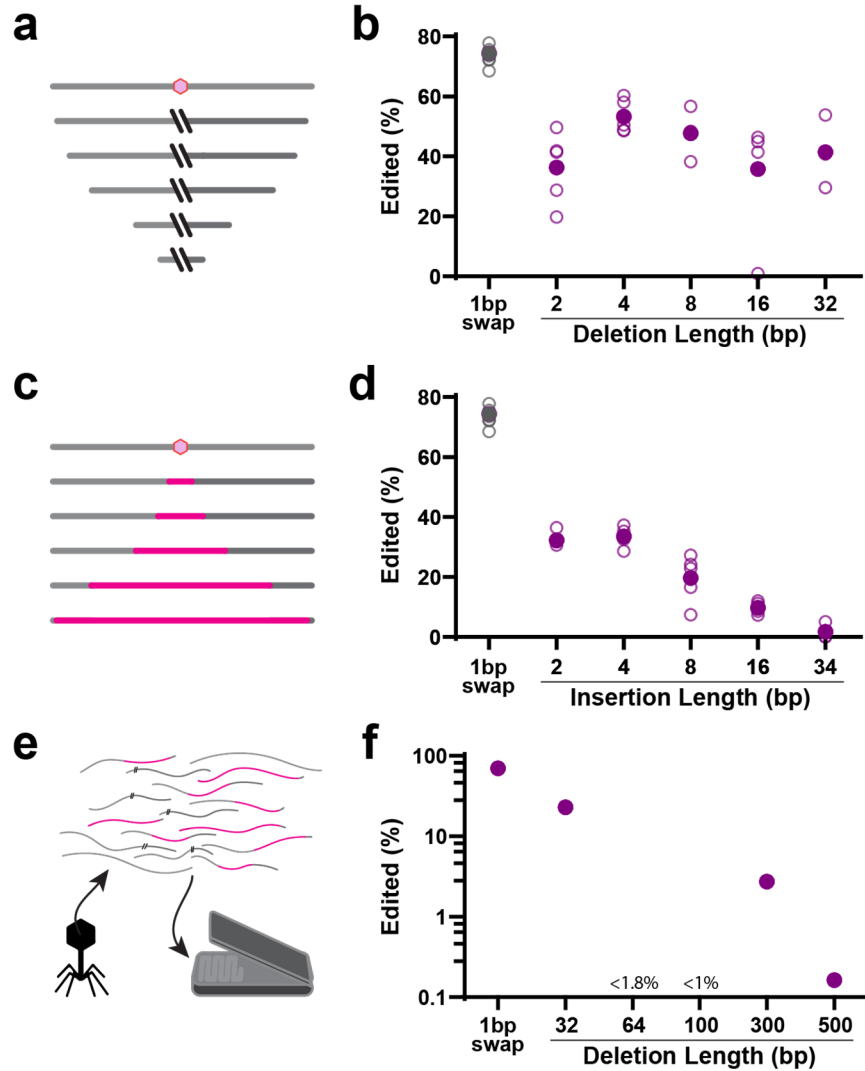
Figure 3. Insertions and Deletions via Recombitrons. a. Schematic of phage genome deletions of increasing size around a common central site (pink hexagon). **b.** Quantification of editing efficiency for deletions preceding position 37,673 as compared to a single base pair synonymous substitution. Five biological replicates are shown in open circles and the mean is shown as a closed circle. There is no significant effect of deletion length (one-way ANOVA, P=0.1564), but all deletions occur at a significantly lower frequency than the single-base substitution (one-way ANOVA, P<0.0001; Dunnett's corrected vs 2 P<0.0001 vs 4 P=0.0083 vs 8 P=0.0008 vs 16 P<0.0001 vs 32 P=0.0005). **c.** Schematic of phage genome insertions of increasing size ending at a common position (pink hexagon). **d.** Quantification of editing efficiency for insertions at position 37,673 as compared to a single base pair synonymous substitution. Five biological replicates are shown in open circles and the mean is shown as a closed circle. Note that the same single base substitution was used as a parallel control for both deletions and insertions and thus the same points are shown here as in b. There is a significant effect of insertion length (one-way ANOVA, P<0.0001), and all insertions occur at a significantly lower frequency than the single-base substitution (one-way ANOVA, P<0.0002; Dunnett's corrected P<0.0001 for all insertions). **e.** Schematic illustrating long-read nanopore quantification. **f.** Quantification of editing efficiency using nanopore sequencing. Points shown represent the fraction of edited reads pooled across three biological replicates. 64 and 100 base pair deletions were not detected in 57 and 102 reads aligned to the edit region, respectively. Additional statistical details in Supplementary Table 1.

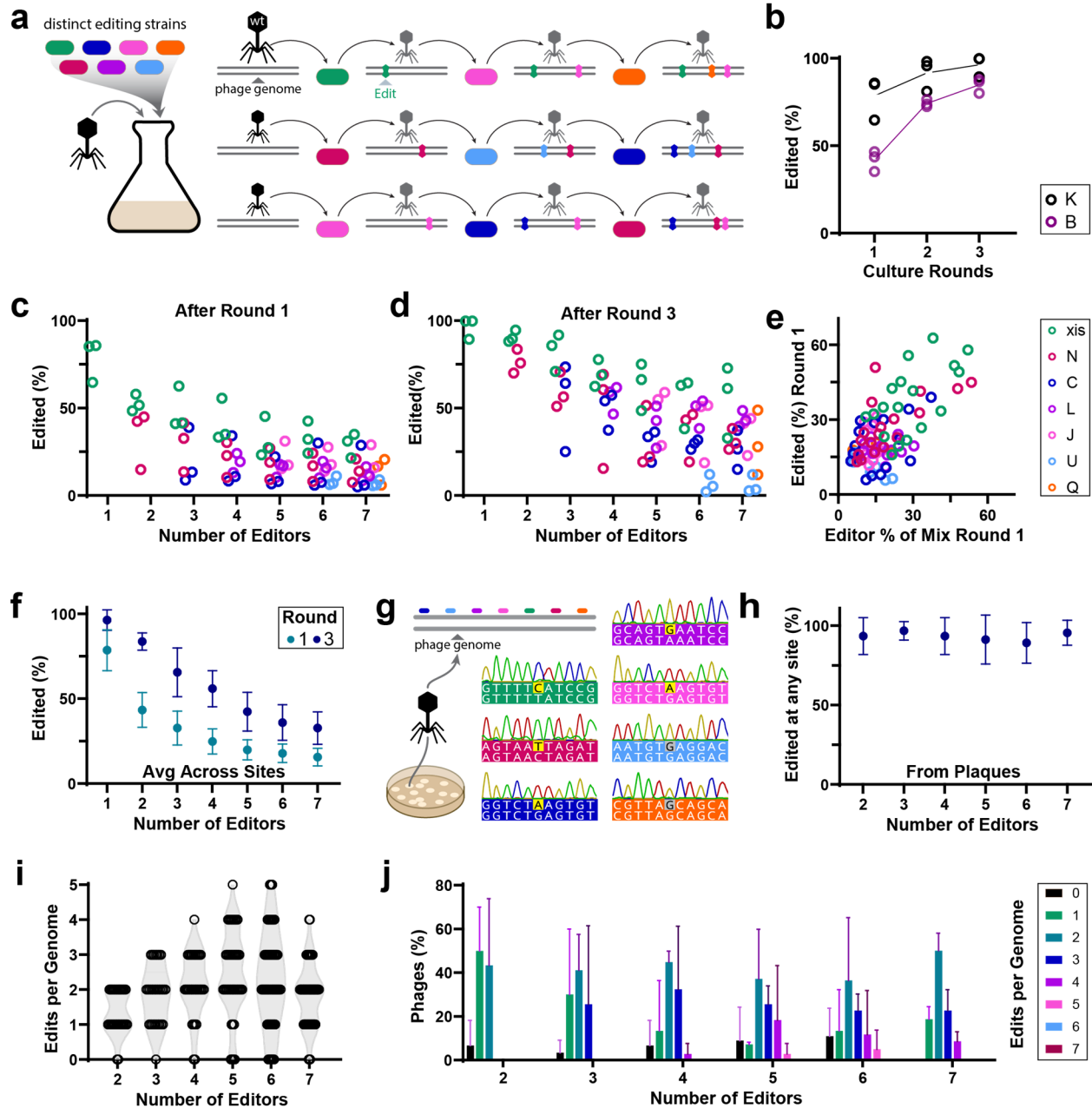**Multiplexed Phage Engineering via Recombitrons**

352

353   One shortcoming of all current phage editing approaches is an inability to simultaneously

354   modify multiple sites in parallel on the same phage. Such parallel modification would be of great

355   benefit to efforts aimed at engineering phages for targeted killing of pathogenic bacteria, but

356   current approaches require cycles of editing, isolation, and re-editing that are impractical in an

357   academic or industrial setting. We reasoned that a slight modification of our recombitron approach

358   would enable such parallel, multiplexed editing of distant sites across a genome. In this

359   modification, multiple bacterial strains that each harbor distinct recombitrons targeting different

360   parts of the phage genome are mixed in a single culture. The phage to be edited is then

361   propagated through that mixed culture. Every new infection event is an opportunity to acquire an

362   edit from one of the recombitrons and, over time, these distinct, distant edits accumulate on

363   individual phage genomes (**Fig 4a**). We ran these experiments in the engineered K-strain, through

364   which the percentage of edited phage genomes increases with additional rounds of editing,

365   beginning at a higher overall rate than the original experiments presented in Figure 1. Editing

366   lambda in this strain yields efficiencies that reach >95% after three rounds of culture (**Fig 4b**).

367   We created seven bacterial editing strains using the lambda recombitrons tested in Figure

368   1b. We then made mixed cultures of 1, 2, 3, 4, 5, 6, or all 7 bacterial strains and performed editing

369   of lambda phage in these mixtures. These strains were grown individually in liquid culture

370   overnight, then separately pre-induced for 2 hours, before being diluted to OD 0.25 and then

371   mixed together in equal proportions. We infected these cultures with lambda (ΔcI) at an MOI of

372   0.1, grew the cultures for 16 hours overnight, and collected the phage lysate the next morning.

373   We then used that phage stock to perform two additional rounds of editing in mixed-host cultures

374   prepared identically to those of the first round. Based on our results that the amount of phage put

375   into the culture is roughly the amount of phage extracted (**Supplementary Fig 1d,e**), we added

376   the same volume of phage in each round based on the titer determination before round one. We

377   quantified editing across phage genomes and genomic loci for each of the mixtures using Illumina

378   sequencing. We found editing across all sites from these mixed cultures after one round and

379   increased editing in all cultures and sites after three rounds (**Fig 4c,d**). We found that the editing

380   rate at any given site across all the mixtures was well correlated with the percentage of that editor

381   in the mixture after round one (**Fig 4e**), and that the overall editing rate across all sites declined

382   with the number of recombitron strains used (**Fig 4f**). This is consistent with a dilution effect of

383   the strains on each other, which suggests that the overall editing rate is limited by the number of

384   cells expressing each recombitron available for the phage to propagate through.

385   While amplicon sequencing showed substantial editing across many sites in a population

386   of phages, we cannot use it to determine whether multiple edits are accumulating on individual

387   phage genomes. Therefore, we plated phages after round three from each condition on bacterial

388   lawns and Sanger sequenced individual plaques at each edit site (**Fig 4g**). This showed that

389   93.2% of phages were edited at one site or more, without employing any form of counter selection

390   (**Fig 4h**). The plaque-based analysis strongly mirrored the Illumina sequencing analysis of editing

391   rate per site by mixture, when plaque data for a condition was pooled (**Supplementary Fig 4**).

392   With the plaque data, however, we can also look at edits per phage genome. We found that

393   multiple sites were edited on a majority of the phages across all conditions, with individual phages

394   edited at up to 5 distinct locations (**Fig 4i,j**). This represents a new milestone in the continuous,

395   multiplexed, selection-free engineering of phage genomes.

396

397

Figure 4. Multiplexed Phage Engineering via Recombitrons a. Schematic illustrating the propagation of phages through cells expressing distinct recombitrons in a co-culture. Over generations of phage propagation, phage genomes accumulate multiple edits from different RT-Donors. **b.** Editing (%) increases over three rounds of editing. Editing in engineered K-strain *E. coli* outperforms the B-strain (two-way ANOVA, strain *P*<0.001, round *P*<0.0001, interaction *P*=0.0282). Three biological replicates are shown in open circles, lines connect averages. **c.** Editing (%) of each site from mixed recombitron cultures after 1 round of editing. Three biological replicates are shown in open circles for each site, clustered over the number of recombitrons used. **d.** Editing (%) of each site from mixed recombitron cultures after 3 rounds of editing, shown as in c. **e.** Editing (%) of each site after 1 round of editing in relation to the proportion of that recombitron strain in the culture (%) (two-tailed Pearson correlation, *P*<0.0001). **f.** Average editing (%) of all sites in each mixed culture. Points represent mean of three biological replicates ±SD (two-way ANOVA, number of editors *P*<0.0001, round *P*<0.0001, interaction *P*=0.234) **g.** Schematic illustrating Sanger

410   sequencing of plaques, which enables quantification of each editing site from clonal phages. Representative
411   data from one plaque with five edits (yellow) and two wild-type sites (grey). Panels **h**, **i**, and **j** are composed
412   of data from three biological replicates. Total plaques: 2 editors, 30 plaques; 3 editors, 29 plaques; 4 editors,
413   31 plaques; 5 editors, 42 plaques; 6 editors, 53 plaques; 7 editors, 55 plaques **h.** Overall editing (%) of any
414   site on plaques isolated from mixed cultures. Points represent mean of three biological replicates ±SD. **i.**
415   Number of edits made on a single phage genome from mixed cultures, by number of recombitrons.
416   Individual plaques from three biological replicates are shown as open circles on a violin plot of distribution.
417   **j.** Number of edits made on a single phage genome from mixed cultures, by number of recombitrons, shown
418   as a histogram (mean ±SD). Additional statistical details in Supplementary Table 1.

419

420   **DISCUSSION**

421   Here we present a new approach to phage editing using recombitrons that leverages

422   modified retrons to continuously provide RT-Donors for recombineering in phage hosts.

423   Recombitrons enable counter-selection-free generation of phage mutants across multiple

424   phages, with optimized forms yielding up to 100% editing efficiency. Moreover, recombitrons can

425   be multiplexed to generate multiple distant mutations on individual phage genomes. Critically, this

426   approach is easy to perform. Recombitrons are generated from simple, standard cloning methods

427   via inexpensive, short oligonucleotides. The process of editing merely requires propagating the

428   bacteria/phage culture, with no intervening transformations or special reagents. Once

429   recombitrons are cloned and phage stocks are prepared, the generation of lambda phage edited

430   at up to five distinct positions required hands-on time of less than 2 hours.

431   This technical advance is poised to change the way we approach innovation in phage

432   biology and phage therapeutics. For instance, studying epistasis in phage genomes becomes a

433   feasible experiment that merely requires mixing recombitron strains in different combinations. The

434   technical hurdle of phage library generation is also dramatically reduced. In our multiplexed

435   experiment, 93.2% of phages were edited. Host range is a major determinant of phage therapy

436   efficacy, which could be addressed by rapidly screening a large library targeting the tail fiber or

437   other critical host range genes for a fraction of the effort of current approaches.

438   Some outstanding questions and further engineering challenges remain. For instance,

439   overexpression of a compatible SSB provided a large benefit to the editing of T7, which

440 demonstrates that recombitrons can be optimized for generality across phages. However, that

441 effect was not immediately transferable to T5. Presumably, T5 may be limited by another phage-

442 specific requirement, and T2 is presumably limited by the use of modified nucleotides. Further

443 work will seek to engineer around these idiosyncrasies and increase the extensibility of this

444 approach to other phages. Finally, in future work we will explore the use of this technology beyond

445 *E. coli* phages.

446

447 **METHODS**

448 Biological replicates were taken from distinct samples, not the same sample measured

449 repeatedly.

450 **Bacterial Strains and Growth Conditions**

451   This work used the following *E. coli* strains: NEB 5-alpha (NEB, C2987; not authenticated),

452 BL21-AI (Thermo Fisher, C607003; not authenticated), bMS.346 and bSLS.114. bMS.346 (used

453 previously[20]) was generated from *E. coli* MG1655 by inactivating the *exoI* and *recJ* genes with

454 early stop codons. bSLS.114 (used previously[29]) was generated from BL21-AI by deleting the

455 retron Eco1 locus by lambda Red recombinase-mediated insertion of an FRT-flanked

456 chloramphenicol resistance cassette, which was subsequently excised using FLP recombinase[42].

457 bCF.5 was generated from bSLS.114, also using the lambda Red system. A 12.1kb region was

458 deleted that contains a partial lambda*B prophage that is native to BL21-AI cells within the attB

459 site, where temperate lambda integrates into the bacterial genome[43].

460   Phage retron recombineering cultures were grown in LB, shaking at 37 °C with appropriate

461 inducers and antibiotics. Inducers and antibiotics were used at the following working

462 concentrations: 2 mg/ml L-arabinose (GoldBio, A-300), 1 mM IPTG (GoldBio, I2481C), 1mM m-

463 toluic acid (Sigma-Aldrich, 202-723-9), 35 µg/ml kanamycin (GoldBio, K-120), 100 µg/ml

464 carbenicillin (GoldBio, C-103) and 25 µg/ml chloramphenicol (GoldBio, C-105; used at 10 µg/ml

465 for selection during bacterial recombineering for strain generation).

466

Plasmid Construction

468 All cloning steps were performed in *E. coli* NEB 5-alpha. pORTMAGE-Ec1 was generated

469 previously (Addgene plasmid no. 138474)[27]. Derivatives of pORTMAGE-Ec1 (pCF.109, pCF.110,

470 pCF.111) were cloned to contain an additional SSB protein, amplified with PCR from its host

471 genome, via Gibson Assembly. Plasmids for RT-Donor production, containing the retron-Eco1 RT

472 and ncRNA with extended a1/a2 regions, were cloned from pSLS.492. pSLS.492 was generated

473 previously (Addgene plasmid no. 184957)[20]. Specific donor sequences for small edits were

474 encoded in primers and substituted into the RT-DNA-encoding region of the ncRNA with a PCR

475 and KLD reaction (NEB M0554). Donor sequences for larger insertions were cloned through

476 Gibson assembly, using synthesized gene fragments (Twist Biosciences). Recombitron ncRNAs

477 encoding the editing donors are listed in **Supplementary Table 2**.

478

Phage Strains and Propagation

480 Phages were propagated from ATCC stocks (Lambda #97538, Lambda WT #23724-B2,

481 T7 #BAA-1025-B2, T5 #11303-B5, T2 #11303-B2) into a 2mL culture of *E. coli* (BL21$^{\Delta Eco1}$) at 37°C

482 at OD600 0.25 in LB medium supplemented with 0.1 mM $MnCl_2$ and 5 mM $MgCl_2$ (MMB) until

483 culture collapse, according to established techniques[44,45]. The culture was then centrifuged for 10

484 min at 4000 rpm and the supernatant was filtered through a 0.2μm filter to remove bacterial

485 remnants. Lysate titer was determined using the full plate plaque assay method as described by

486 Kropinski et al.[46]. We used recombitrons to edit this lambda strain to encode two early stop codons

487 in the cI gene, responsible for lysogeny control, to ensure the phage was strictly lytic (lambda

488 ΔcI). After recombineering, we Sanger sequenced plaques to check the edit sites. We isolated an

489 edited plaque and used Illumina Miseq of its lysate to ensure purity of the edited phage. We used

490 this strictly lytic version for all experiments involving lambda phage, unless otherwise noted.

491   Genomic locations used to label edits are from wild-type reference sequences of phages

492   available through NCBI GenBank: lambda (J02459.1), T5 (AY587007.1), T7 (V01146.1), and T2

493   (AP018813.1). We found that the strain of phage lambda we used naturally contains a large

494   genomic deletion between 21738 and 27723. This region encodes genes that are not well-

495   characterized, but may be involved in lysogeny control[47,48].

496

497   **Plaque Assays**

498   Small drop and full plate plaque assays were performed as previously described by

499   Mazzocco et al.[49], starting from bacteria grown overnight at 37°C. For small drop plaque assays,

500   200ul of the bacterial culture was mixed with 2mL melted MMB agar (LB + 0.1 mM $MnCl_2$ + 5 mM

501     $MgCl_2$ + 0.75% agar) and plated on MMB agar plates. 10-fold serial dilutions in MMB were

502   performed for each of the phages and 2ul drops were placed on the bacterial layer. The plates

503   were dried for 20 min at room temperature and then incubated overnight at 37°C. Full plate plaque

504   assays were set up by mixing 200ul of the bacterial culture with 20ul of phage lysate, using 10-

505   fold serial dilutions of the lysate to achieve between 200-10 plaques. After incubating at room

506   temperature without shaking for 5 min, the mixture was added to 2mL melted MMB agar and

507   poured onto MMB agar plates. The plates were dried for 20 min at room temperature and

508   incubated overnight at 37°C. Plaque forming units were counted to calculate the titer.

509

510   **Recombineering and Sequencing**

511   The retron cassette, with modified ncRNA to contain a donor, was co-expressed with

512   CspRecT and mutL E32K from the plasmid pORTMAGE-Ec1. All experiments, except

513   multiplexing and large insertions/deletions (>30 bp), were conducted in 500uL cultures in a deep

514   96-well plate. Multiplexing experiments were conducted in 3mL cultures in 15mL tubes. For

515   amplification-free sequencing by nanopore, larger culture volumes (25mL cultures in 250 mL

516   flasks) were used to enable collection of a higher quantity of phage DNA. Cultures were induced

517   for 2 hrs at 37 °C, with shaking. The OD600 of each culture was measured to approximate cell

518   density and cultures were diluted to OD600 0.25. Phages were originally propagated through the

519   corresponding host that would be used for editing (B- or K-strain E coli). A volume of pre-titered

520   phage was added to the culture to reach a multiplicity of infection (MOI) of 0.1. The infected culture

521   was grown overnight for 16 hrs, before being centrifuged for 10 min at 4000 rpm to remove the

522   cells. The supernatant was filtered through a 0.2μm filter to isolate phage.

523   For amplicon-based sequencing, the lysate was mixed 1:1 with DNase/RNase-free water

524   and the mixture was incubated at 95°C for 5 min. This boiled culture (0.25ul) was used as a

525   template in a 25ul PCR reaction with primers flanking the edit site on the phage genome. These

526   amplicons were indexed and sequenced on an Illumina MiSeq instrument. Sequencing primers

527   are listed in **Supplementary Table 3**.

528   For amplification-free sequencing, extracellular DNA was removed through DNase I

529   treatment, with 20 U of DNase I (NEB, M0303S) for 1mL of phage lysate, incubated at room

530   temperature for 15 min and then inactivated at 75°C for 5 min. Phage were then lysed and DNA

531   extracted using the Norgen Phage DNA Isolation Kit (Norgen, 46800). The samples were prepped

532   for sequencing in a standard Nanopore workflow. DNA ends were repaired using NEBNext Ultra

533   II End Repair/dA-Tailing Module (NEB, E7526S). End-repaired DNA was then cleaned up using

534   Ampure XP beads. Barcodes were ligated using the standard protocol for Nanopore Barcode

535   Expansion Kit (Oxford Nanopore Technologies, EXP-NBD196). After barcoding, the standard

536   Oxford Nanopore adaptor ligation, clean-up, and loading protocols were followed for Ligation

537   Sequencing Kit 109 and Flow Cell 106 for the MinION instrument (Oxford Nanopore

538   Technologies, SQK-LSK109, FLO-MIN106D). Base calling was performed using Guppy

539   Basecaller with high accuracy and barcode trimming settings.

540   Sanger sequencing of phage plaques was accomplished by picking plaques produced

541   from the full plate assay described above. Plates were sent to Azenta/Genewiz for sequencing

542 with one of the MiSeq-compatible primers used to assess the same site. Sequences were

543 analyzed using Geneious through alignment to the region surrounding the edit site on the phage

544 genome.

545

546 **Editing Rate Quantification**

547 A custom Python workflow was used to quantify edits from amplicon sequencing data.

548 Reads were required to contain outside flanking nucleotide sequences that occur on the phage

549 genome, but beyond the RT-Donor region to avoid quantifying RT-DNA or plasmid. Reads were

550 then trimmed by left and right sequences immediately flanking the edit site. Reads containing

551 these inside flanking sequences in the correct order with an appropriate distance between them

552 (depending on edit type) were assigned to either wild-type, edit, or other. The edit percentage is

553 the number of edited reads over the sum of all reads containing flanking sequences.

554 A distinct custom Python program was used for quantifying amplification-free nanopore

555 sequencing data, due to the higher error rates in nanopore sequencing and the lack of a defined

556 region of the genome contained in each read. Reads were aligned using BLAST+ to three

557 reference genomes: wild-type lambda, edited lambda containing the matching edit to the read's

558 experiment, and BL21-AI *E. coli*. If reads aligned to either lambda genomes, the read's alignment

559 coordinates had to be at least 50 bases past the insertion/deletion coordinates, as well as be >

560 500 bp and have >50% of the read mapped to the reference genome as quality scores. If a read

561 aligned to the insertion/deletion point and passed all quality scores, the percent identity and

562 alignment length over read length were compared to assign the read as either wild-type or edited.

563 Coverage of the edit region was 50-1000x per experimental condition.

564

565 **Data Availability**

566　All data supporting the findings of this study are available within the article and its supplementary

567　information, or will be made available from the authors upon request. Sequencing data associated

568　with this study are available in the NCBI SRA (PRJNA933262).

569

570　**Code Availability**

571　Custom code to process or analyze data from this study will be made available on GitHub prior to

572　peer-reviewed publication.

573

574　**Acknowledgements**

580

581　**Author Contributions**

582　C.B.F., S.B.-K., and S.L.S. conceived the study and, with K.D.C., K.A.Z., and A.G.-D., outlined

583　the scope of the project and designed experiments. C.B.F. developed phage handling and editing

584　protocols. Experiments were performed and analyzed by C.B.F. (Fig1 e-h, Fig2, Fig4, Supp Fig1

585　b-h, Supp Fig2, Supp Fig4), K.D.C. (Fig3, Supp Fig3), S.B.-K. (Fig1 b-d, Supp Fig1 a), and K.A.Z

586　(Fig3, Supp Fig3). C.B.F. and S.L.S. wrote the manuscript, with input from all authors.

587

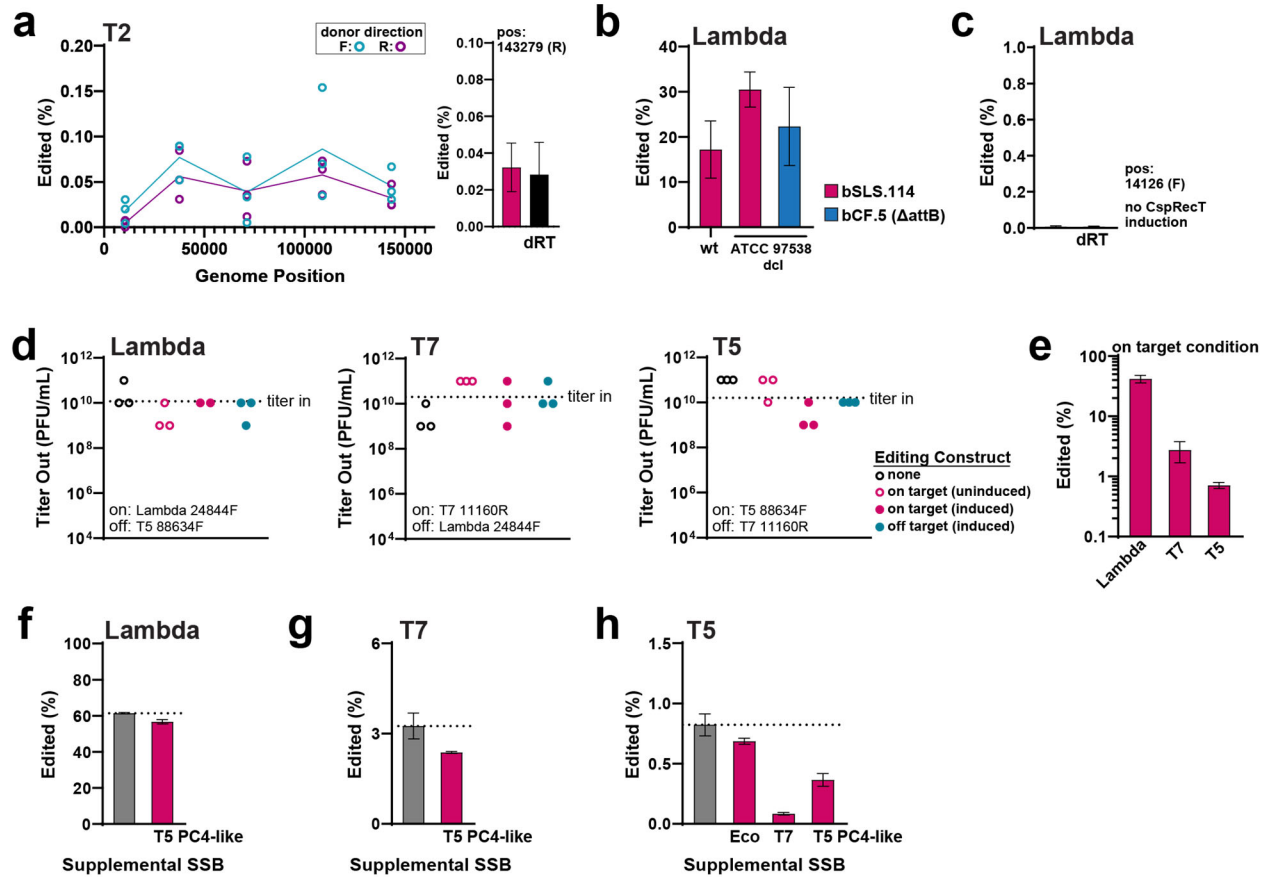588　**Competing Interests**

589　C.B.F., S.B.K., and S.L.S. are named inventors on a patent application related to the technologies

590　described in this work.

591

592   **CORRESPONDING AUTHOR**

593   Correspondence to Seth L. Shipman.

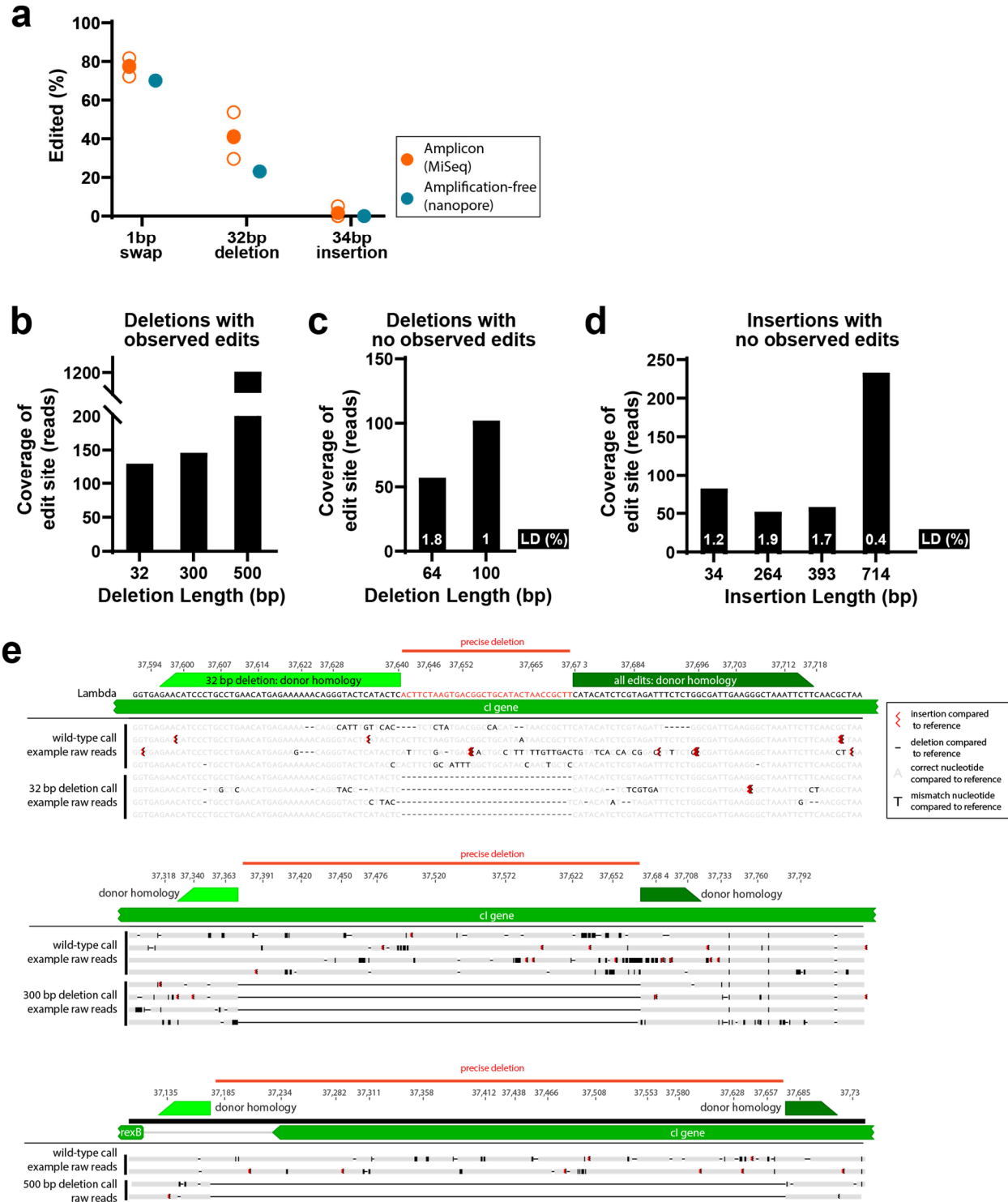594   **Supplementary Figures**

595

596   **Supplementary Figure 1. Accompaniment to Figure 1. a.** Left: Edited phage genomes (as a % of all
597   genomes) across phage T2. Editing with a forward RT-DNA is shown in blue, reverse in purple. Three
598   individual replicates are shown in open circles at each point. Right: Editing with the recombitron at site
599   143,279 (R) (±SD) versus a dRT control. **b.** Editing (%) of lambda and lambda_ΔcI in different host strains
600   at site 14,070 (R). Mean ±SD is shown for 3 (wt in bSLS.114), 5 (ΔcI in bSLS.114), and 2 (ΔcI in bCF.5)
601   biological replicates. **c.** Editing (%) of lambda without induction of CspRecT. Mean ±SD for 3 biological
602   replicates at site 14,126. **d.** Titer (PFU/mL) of phage lambda, T7, and T5 after propagation through host
603   cells of different conditions, compared to amount of phage added to the culture. Host conditions are without
604   recombitrons (open black circles), with uninduced recombitrons (open pink circles), with induced
605   recombitrons (closed pink circles), and with induced recombitrons that target a different phage (closed blue
606   circles). Individual biological replicates are shown in circles for each condition. **e.** Editing (%) of phage
607   lambda, T7, and T5 from the induced, on-target recombitron condition in panel d. **f.** Editing (%) of lambda
608   at site 14126 (F) compared to editing with supplemental expression of T5 SSB. **g.** Editing (%) of T7 at site
609   22872 (R) compared to editing with supplemental expression of T5 SSB. **h.** Editing (%) of T5 at site 88634
610   (F) with supplemental expression of *E. coli* SSB, T7 SSB, or T5 SSB.

611
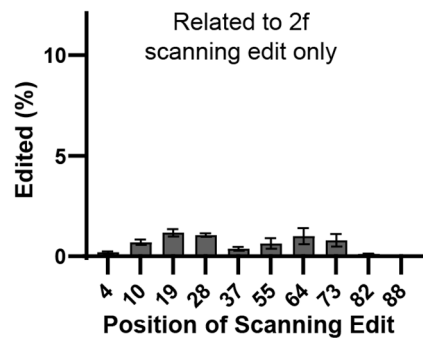
Supplementary Figure 2. Accompaniment to Figure 2. Rate of acquiring only the scanning edit in lambda when donors contain both scanning and central edits. (mean ±SD).

612
613
614

Supplementary Figure 3. Accompaniment to Figure 3. a. Comparison of edited phages measure by amplicon (Illumina) or amplification-free (Oxford Nanopore) sequencing. Open orange circles represent biological replicates of amplicon data and filled orange circle represents the mean. Filled blue circle represents the aggregate nanopore data from three replicates. **b.** Coverage of the editing site in long-read nanopore sequencing for deletions in which we observe editing. **c.** Coverage of the editing site in long-read nanopore sequencing for deletions in which we do not observe any edits. Estimated limit of detection for

621 these samples is calculated by dividing 100 by the coverage of the site. **d.** Coverage of the editing site in
622 long-read nanopore sequencing for large insertions, for which we do not observe any edits. Estimated limit
623 of detection for these samples is calculated by dividing 100 by the coverage of the site. **e.** Examples of
624 nanopore reads for different deletion conditions.
625
626
627

After Round 3: Plaques
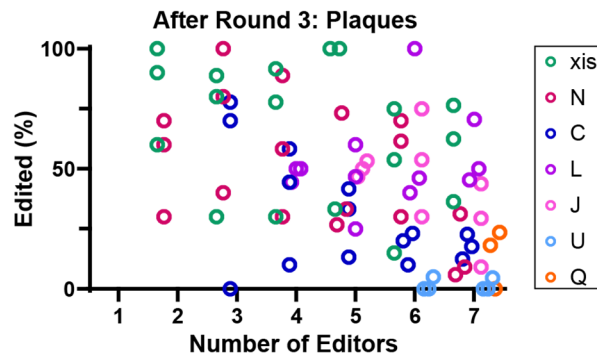
628 **Supplementary Figure 4. Accompaniment to Figure 4.** Editing (%) from Sanger sequencing of plaques
629 at each site from mixed recombitron cultures after 3 rounds of editing. Three biological replicates are shown
630 in open circles for each site, clustered over the number of recombitrons used.

631 ## **References:**
632

633 1   Strathdee, S. A., Hatfull, G. F., Mutalik, V. K. & Schooley, R. T. Phage therapy: From biological
634   mechanisms to future directions. *Cell* **186**, 17-31, doi:10.1016/j.cell.2022.11.017 (2023).
635 2   Mahler, M., Costa, A. R., van Beljouw, S. P. B., Fineran, P. C. & Brouns, S. J. J. Approaches for
636   bacteriophage genome engineering. *Trends in biotechnology*, doi:10.1016/j.tibtech.2022.08.008
637   (2022).
638 3   Simon, A. J., Ellington, A. D. & Finkelstein, I. J. Retrons and their applications in genome
639   engineering. *Nucleic Acids Res* **47**, 11007-11019, doi:10.1093/nar/gkz865 (2019).
640 4   Żaczek, M., Weber-Dąbrowska, B., Międzybrodzki, R., Łusiak-Szelachowska, M. & Górski, A.
641   Phage Therapy in Poland - a Centennial Journey to the First Ethically Approved Treatment
642   Facility in Europe. *Frontiers in microbiology* **11**, 1056, doi:10.3389/fmicb.2020.01056 (2020).
643 5   Global burden of bacterial antimicrobial resistance in 2019: a systematic analysis. *Lancet*
644   *(London, England)* **399**, 629-655, doi:10.1016/s0140-6736(21)02724-0 (2022).
645 6   O'Neill, J. Tackling drug-resistant infections globally: final report and recommendations. (2016).
646 7   Chan, B. K., Stanley, G., Modak, M., Koff, J. L. & Turner, P. E. Bacteriophage therapy for
647   infections in CF. *Pediatric pulmonology* **56 Suppl 1**, S4-s9, doi:10.1002/ppul.25190 (2021).
648 8   Schooley, R. T. *et al.* Development and Use of Personalized Bacteriophage-Based Therapeutic
649   Cocktails To Treat a Patient with a Disseminated Resistant Acinetobacter baumannii Infection.
650   *Antimicrobial agents and chemotherapy* **61**, doi:10.1128/aac.00954-17 (2017).
651 9   Kiro, R., Shitrit, D. & Qimron, U. Efficient engineering of a bacteriophage genome using the type
652   I-E CRISPR-Cas system. *RNA biology* **11**, 42-44, doi:10.4161/rna.27766 (2014).
653 10   Box, A. M., McGuffie, M. J., O'Hara, B. J. & Seed, K. D. Functional Analysis of Bacteriophage
654   Immunity through a Type I-E CRISPR-Cas System in Vibrio cholerae and Its Application in

Bacteriophage Genome Engineering. *Journal of bacteriology* **198**, 578-590, doi:10.1128/jb.00747-15 (2016).

11   Bari, S. M. N., Walker, F. C., Cater, K., Aslan, B. & Hatoum-Aslan, A. Strategies for Editing Virulent Staphylococcal Phages Using CRISPR-Cas10. *ACS Synth Biol* **6**, 2316-2325, doi:10.1021/acssynbio.7b00240 (2017).

12   Ramirez-Chamorro, L., Boulanger, P. & Rossier, O. Strategies for Bacteriophage T5 Mutagenesis: Expanding the Toolbox for Phage Genome Engineering. *Frontiers in microbiology* **12**, 667332, doi:10.3389/fmicb.2021.667332 (2021).

13   Adler, B. A. *et al.* Broad-spectrum CRISPR-Cas13a enables efficient phage genome editing. *Nature microbiology* **7**, 1967-1979, doi:10.1038/s41564-022-01258-x (2022).

14   Strotskaya, A. *et al.* The action of Escherichia coli CRISPR-Cas system on lytic bacteriophages with different lifestyles and development strategies. *Nucleic Acids Res* **45**, 1946-1957, doi:10.1093/nar/gkx042 (2017).

15   Ando, H., Lemire, S., Pires, D. P. & Lu, T. K. Engineering Modular Viral Scaffolds for Targeted Bacterial Population Editing. *Cell systems* **1**, 187-196, doi:10.1016/j.cels.2015.08.013 (2015).

16   Emslander, Q. *et al.* Cell-free production of personalized therapeutic phages targeting multidrug-resistant bacteria. *Cell chemical biology* **29**, 1434-1445.e1437, doi:10.1016/j.chembiol.2022.06.003 (2022).

17   Farzadfard, F. & Lu, T. K. Genomically encoded analog memory with precise in vivo DNA writing in living cell populations. *Science* **346**, 1256272-1256272, doi:10.1126/science.1256272 (2014).

18   Schubert, M. G. *et al.* High-throughput functional variant screens via in vivo production of single-stranded DNA. *PNAS* **118**, e2018181118, doi:10.1073/pnas.2018181118 (2021).

19   Simon, A. J., Morrow, B. R. & Ellington, A. D. Retroelement-Based Genome Editing and Evolution. *ACS Synth. Biol.* **7**, 2600-2611, doi:10.1021/acssynbio.8b00273 (2018).

20   Lopez, S. C., Crawford, K. D., Lear, S. K., Bhattarai-Kline, S. & Shipman, S. L. Precise genome editing across kingdoms of life using retron-derived DNA. *Nat Chem Biol* **18**, 199-206, doi:10.1038/s41589-021-00927-y (2022).

21   Bobonis, J. *et al.* Bacterial retrons encode phage-defending tripartite toxin-antitoxin systems. *Nature* **609**, 144-150, doi:10.1038/s41586-022-05091-4 (2022).

22   Millman, A. *et al.* Bacterial Retrons Function In Anti-Phage Defense. *Cell* **183**, 1551-1561.e1512, doi:10.1016/j.cell.2020.09.065 (2020).

23   Palka, C., Fishman, C. B., Bhattarai-Kline, S., Myers, S. A. & Shipman, S. L. Retron reverse transcriptase termination and phage defense are dependent on host RNase H1. *Nucleic Acids Res* **50**, 3490-3504, doi:10.1093/nar/gkac177 (2022).

24   Gao, L. *et al.* Diverse enzymatic activities mediate antiviral immunity in prokaryotes. *Science* **369**, 1077-1084, doi:10.1126/science.aba0372 (2020).

25   Mosberg, J. A., Lajoie, M. J. & Church, G. M. Lambda red recombineering in Escherichia coli occurs through a fully single-stranded intermediate. *Genetics* **186**, 791-799, doi:10.1534/genetics.110.120782 (2010).

26   Nyerges, Á. *et al.* A highly precise and portable genome engineering method allows comparison of mutational effects across bacterial species. *Proceedings of the National Academy of Sciences of the United States of America* **113**, 2502-2507, doi:10.1073/pnas.1520040113 (2016).

27   Wannier, T. M. *et al.* Improved bacterial recombineering by parallelized protein discovery. *Proceedings of the National Academy of Sciences of the United States of America* **117**, 13689-13698, doi:10.1073/pnas.2001588117 (2020).

28   Nyerges, Á. *et al.* Conditional DNA repair mutants enable highly precise genome engineering. *Nucleic Acids Res* **42**, e62, doi:10.1093/nar/gku105 (2014).

29   Bhattarai-Kline, S. *et al.* Recording gene expression order in DNA by CRISPR addition of retron barcodes. *Nature* **608**, 217-225, doi:10.1038/s41586-022-04994-6 (2022).

30   Aronshtam, A. & Marinus, M. G. Dominant negative mutator mutations in the mutL gene of Escherichia coli. *Nucleic Acids Res* **24**, 2498-2504, doi:10.1093/nar/24.13.2498 (1996).

31   Weigele, P. & Raleigh, E. A. Biosynthesis and Function of Modified Bases in Bacteria and Their Viruses. *Chemical reviews* **116**, 12655-12687, doi:10.1021/acs.chemrev.6b00114 (2016).

32   Weigel, C. & Seitz, H. Bacteriophage replication modules. *FEMS microbiology reviews* **30**, 321-381, doi:10.1111/j.1574-6976.2006.00015.x (2006).

33   Wolfson, J., Dressler, D. & Magazin, M. Bacteriophage T7 DNA replication: a linear replicating intermediate (gradient centrifugation-electron microscopy-E. coli-DNA partial denaturation). *Proceedings of the National Academy of Sciences of the United States of America* **69**, 499-504, doi:10.1073/pnas.69.2.499 (1972).

34   Bourguignon, G. J., Sweeney, T. K. & Delius, H. Multiple origins and circular structures in replicating T5 bacteriophage DNA. *Journal of virology* **18**, 245-259, doi:10.1128/jvi.18.1.245-259.1976 (1976).

35   Hochschild, A. & Lewis, M. The bacteriophage lambda CI protein finds an asymmetric solution. *Current opinion in structural biology* **19**, 79-86, doi:10.1016/j.sbi.2008.12.008 (2009).

36   Tal, A., Arbel-Goren, R., Costantino, N., Court, D. L. & Stavans, J. Location of the unique integration site on an Escherichia coli chromosome by bacteriophage lambda DNA in vivo. *Proceedings of the National Academy of Sciences of the United States of America* **111**, 7308-7312, doi:10.1073/pnas.1324066111 (2014).

37   Filsinger, G. T. *et al.* Characterizing the portability of phage-encoded homologous recombination proteins. *Nat Chem Biol* **17**, 394-402, doi:10.1038/s41589-020-00710-5 (2021).

38   Hernandez, A. J. & Richardson, C. C. Gp2.5, the multifunctional bacteriophage T7 single-stranded DNA binding protein. *Seminars in cell & developmental biology* **86**, 92-101, doi:10.1016/j.semcdb.2018.03.018 (2019).

39   Werten, S. Identification of the ssDNA-binding protein of bacteriophage T5: Implications for T5 replication. *Bacteriophage* **3**, e27304, doi:10.4161/bact.27304 (2013).

40   Marinelli, L. J. *et al.* BRED: a simple and powerful tool for constructing mutant and recombinant bacteriophage genomes. *PLOS ONE* **3**, e3957, doi:10.1371/journal.pone.0003957 (2008).

41   Mosberg, J. A., Gregg, C. J., Lajoie, M. J., Wang, H. H. & Church, G. M. Improving Lambda Red Genome Engineering in Escherichia coli via Rational Removal of Endogenous Nucleases. *PLOS ONE* **7**, e44638, doi:10.1371/journal.pone.0044638 (2012).

42   Datsenko, K. A. & Wanner, B. L. One-step inactivation of chromosomal genes in Escherichia coli K-12 using PCR products. *PNAS* **97**, 6640-6645, doi:10.1073/pnas.120163297 (2000).

43   Jeong, H., Kim, H. J. & Lee, S. J. Complete Genome Sequence of Escherichia coli Strain BL21. *Genome announcements* **3**, doi:10.1128/genomeA.00134-15 (2015).

44   Doron, S. *et al.* Systematic discovery of antiphage defense systems in the microbial pangenome. *Science* **359**, doi:10.1126/science.aar4120 (2018).

45   Fortier, L. C. & Moineau, S. Phage production and maintenance of stocks, including expected stock lifetimes. *Methods in molecular biology (Clifton, N.J.)* **501**, 203-219, doi:10.1007/978-1-60327-164-6_19 (2009).

46   Kropinski, A. M., Mazzocco, A., Waddell, T. E., Lingohr, E. & Johnson, R. P. Enumeration of bacteriophages by double agar overlay plaque assay. *Methods in molecular biology (Clifton, N.J.)* **501**, 69-76, doi:10.1007/978-1-60327-164-6_7 (2009).

47   Rajagopala, S. V., Casjens, S. & Uetz, P. The protein interaction map of bacteriophage lambda. *BMC microbiology* **11**, 213, doi:10.1186/1471-2180-11-213 (2011).

749 48   Epp, C., Pearson, M. L. & Enquist, L. Downstream regulation of int gene expression by the b2
750   region in phage lambda. *Gene* **13**, 327-337, doi:10.1016/0378-1119(81)90012-3 (1981).
751 49   Mazzocco, A., Waddell, T. E., Lingohr, E. & Johnson, R. P. Enumeration of bacteriophages using
752   the small drop plaque assay system. *Methods in molecular biology (Clifton, N.J.)* **501**, 81-85,
753   doi:10.1007/978-1-60327-164-6_9 (2009).

754